
Article:
Lim, A.J., Falle, S.A.E.G. and Hartquist, T.W. (2005) The production of magnetically dominated star-forming regions. The Astrophysical Journal, 632 (2). L91-L94. ISSN: 0004-637X

The Astrophysical Journal, 632:L91–L94, 2005 October 20

THE PRODUCTION OF MAGNETICALLY DOMINATED STAR-FORMING REGIONS

A. J. Lim,[1] S. A. E. G. Falle,[2] and T. W. Hartquist[1]

Received 2005 February 7; accepted 2005 September 14; published 2005 October 12

ABSTRACT

We consider the dynamical evolution of an interstellar cloud that is initially in thermal equilibrium in the warm phase and is then subjected to a sudden increase in the pressure of its surroundings. We find that if the initial plasma β of the cloud is of order unity, then there is a considerable period during which the material in the cloud both has a small β and is in the thermally unstable temperature range. These conditions are not only consistent with observations of star-forming regions but also ideally suited to the production of density inhomogeneities by magnetohydrodynamic waves. The end result should be a cloud whose size and average density are typical of Giant Molecular Clouds (GMCs) and that contains denser regions whose densities are in the range inferred for the translucent clumps in GMCs.

Subject heading: MHD

1. INTRODUCTION

Observations of magnetic fields in star-forming regions (e.g., Crutcher 1999) tell us that the plasma β is of order 0.04 and that the velocity dispersion is of the order of the Alfvén speed. For this reason, many of the simulations of the early stages of star formation (e.g., Fiedler & Mouschovias 1993; Ballesteros-Paredes & Mac Low 2002; Falle & Hartquist 2002; Padoan & Nordlund 2002; Gammie et al. 2003) have assumed that the initial value of β is low. These papers show that dense structures can be formed under these conditions, but they do not consider how β came to be so low in the first place.

On scales large compared to the separation between clouds, the thermal and magnetic pressures in the interstellar medium are comparable. Locally β may be about 0.5, while in the midplane at a distance of 5 kpc from the Galactic center it may be about 1.5 (Ferriere 1998). The production of a star-forming region must therefore also reduce β by a considerable factor. Here we examine a mechanism for this that relies on pressure-driven compression and radiative cooling.

This process produces a transient structure, but this is not in conflict with estimates of only a few million years for the ages of the stars in Giant Molecular Clouds (GMCs) (Ballesteros-Paredes et al. 1999; Hartman 2003). This is also not very different from the time that a clump moving at the observed velocities of $\sim$10 km s^{-1} takes to travel a significant fraction of the size of a GMC ($\sim$100 pc). We therefore assume that GMCs are transient and that their formation is triggered by external disturbances. We make no attempt to follow the entire evolution of a GMC; instead we describe an idealized numerical calculation that illustrates how a cloud might make the transition from a state with moderate β to one with low β.

A significant fraction of interstellar space is filled by 10^6 K gas, which is composed of overlapping supernova remnants (Cox & Smith 1974; McKee & Ostriker 1977). This gas is continually being reheated by shocks from supernova explosions. One estimate (McKee & Ostriker 1977) indicates that, on average, this causes the pressure at any given point to fluctuate significantly on timescales of the order of a million years or less. Such pressure fluctuations also appear in simulations of the structure of the interstellar medium (e.g., Gazol-Patiño & Passot 1999; Korpi et al. 1999; de Avillez & Breitschwerdt 2004, 2005; Mac Low et al. 2005). De Avillez & Breitschwerdt (2005) and Mac Low et al. (2005) do, indeed, find low-β regions in their simulations. However, these are global simulations containing a number of ingredients, so that it is not entirely clear how these regions are produced. Our idealized calculation not only has the advantage that the mechanism is clear but also makes it possible to use higher resolution than is possible in a global simulation. As seen below, even this higher resolution is not sufficient to follow the entire evolution accurately.

2. THE MODEL

2.1. *Heating and Cooling*

For the heating and cooling rates appropriate for diffuse atomic gas, there are two thermally stable phases that can be in pressure equilibrium with each other for a range of thermal pressures. The low-density warm phase is at $\sim 10^4$ K, while the high-density cold phase is at $\sim 10^2$ K. If molecules form, as they do in the clumps within GMCs, then the temperature of the cold stable phase decreases. The thermal pressure in the warm phase has a maximum above which only the cold phase can be in thermal equilibrium.

As a simple model of the thermal behavior of the material in the cloud we adopt the following form for the net heating rate per unit volume:

$$H = \rho[0.015 - \rho\Lambda(T)] \text{ ergs cm}^{-3} \text{ s}^{-1},$$

where

$$\Lambda(T) = \begin{cases} 3.564 \times 10^{16} T^{2.12}, & 0 \text{ K} \le T < 141 \text{ K}, \\ 9.1 \times 10^{18} T, & 141 \text{ K} \le T < 313 \text{ K}, \\ 1.14 \times 10^{20} T^{0.56}, & 313 \text{ K} \le T < 6102 \text{ K}, \\ 1.924 \times 10^{8} T^{3.67}, & 6102 \text{ K} \le T < 10^5 \text{ K}, \\ 1.362 \times 10^{29} T^{-0.5}, & T \ge 10^5 \text{ K} \end{cases}$$

(Sánchez-Salcedo et al. 2002). H is of the same form as that appropriate for the diffuse atomic gas (Wolfire et al. 1995). If

[1] School of Physics and Astronomy, University of Leeds, Leeds LS2 9JT, UK.
[2] Department of Applied Mathematics, University of Leeds, Woodhouse Lane, Leeds LS2 9JT, UK.

we ignore the dependence of the ionization fraction on temperature, then the pressure is

$$p = \frac{\rho k T}{m},$$

where $m = 2 \times 10^{-24}$ g is the mean particle mass. For this model, the maximum density and pressure of the warm phase in thermal equilibrium are 0.5 cm^{-3} and 3051k, respectively. Here k is Boltzmann's constant.

2.2. *Initial Conditions*

It is well known that a transition from the warm to the cold phase can be triggered by a relatively small pressure increase caused by either flow convergence (Hennebelle & Pérault 1999, 2000) or a weak shock (Koyama & Inutsuka 2000, 2002, 2004). If β is initially of order unity, then this transition can produce a small value of β. We therefore consider a cloud that is initially in the warm phase and in pressure equilibrium with the surrounding hotter material. The hot gas can be assumed to be adiabatic, but both heating and radiative cooling are important within the cloud. We then suppose that the cloud is subjected to an increase in the pressure of the surrounding hot material from a value at which the warm phase exists to one at which it does not. The pressure increase is assumed to take place on a timescale that is short compared to the time required for the cloud to adjust.

In all the calculations, the cloud is initially in thermal equilibrium in the warm phase with a number density of 0.45 cm^{-3}, corresponding to a temperature of 6277 K and a pressure of 2825k. The external pressure is imposed by embedding the cloud in uniform hot material with density 0.01 cm^{-3} with the appropriate pressure. This material is not in thermal equilibrium, but its cooling time is so long that it can be assumed to behave adiabatically. The initial magnetic field is in the axial direction and is uniform everywhere with a pressure equal to the thermal pressure in the cloud, i.e., $\beta = 1$ in the cloud. Since the cloud is initially spherical, the flow remains axisymmetric. Table 1 lists the external pressure and size of the cloud for the five cases considered. Changing the cloud radius only affects the ratio of cloud radius to the cooling length behind the fast-mode shock that propagates into the cloud. This ratio is $\simeq$0.1 for a cloud radius of 200 pc. Note that the external thermal pressures are well within the range found in global simulations.

Model E explores the effect of an external thermal pressure, p_e, that decreases with time according to

$$p_e = \begin{cases} p_0 e^{-t/t_c}, & p_e > p_0, \\ p_0, & \text{otherwise.} \end{cases}$$

Here $p_0 = 10{,}000k$ is the initial external thermal pressure and $t_c = 2.6 \times 10^7$ yr, which is approximately twice the time it takes the fast shock to return to the edge of the cloud (see § 2.4).

2.3. *Computational Details*

All the calculations were done in axisymmetry using the unstructured hierarchical adaptive grid code described in Falle & Giddings (1993). This uses a hierarchy of grids $G^0, \ldots, G^N$ such that the mesh spacing on grid G^n is $\Delta x_0/2^n$. Grids G^0 and G^1 cover the whole domain, but the finer grids only exist where they are needed. The solution at each position is calculated on all grids that exist there, and the difference between these solutions is used to control refinement. In order to ensure Courant number matching at the boundaries between coarse and fine grids, the time step on grid G^n is $\Delta t_0/2^n$, where Δt_0 is the time step on G^0. Such a grid structure is very efficient for flows that contain very thin dense regions since it confines the fine grids to where they are needed. The basic algorithm is an MHD version of the second-order Godunov scheme described in Falle (1991). This uses a linear Riemann solver and the divergence cleaning algorithm described in Dedner et al. (2002).

TABLE 1
External Pressure and Cloud Radius

Model	External Gas Pressure	Cloud Radius (pc)
A	15000k	200
B	10000k	200
C	10000k	50
D	7500k	200
E[a]	10000k	200

[a] Decreasing external pressure.

The computational domain is $0 \le r \le 2R_c$, $0 \le z \le 2R_c$, where R_c is the cloud radius. The boundary conditions are symmetry on the $z = 0$ plane and the axis and free flow conditions elsewhere. The low density in the external gas ensures that the boundaries at $r = 2R_c$ and $z = 2R_c$ have a negligible effect on the solution. There were six grid levels with the finest being 1280 × 1280. This gives a mesh spacing of 0.31 pc for models A, C, D, and E and 0.08 pc for model B. Even though this is significantly higher resolution than that attained by de Avillez & Breitschwerdt (2005) and Mac Low et al. (2005), it is not sufficient to follow the complete evolution of the cloud. It is, however, enough to show the formation of the fragments that we identify with the translucent clumps and to give some insight into their initial evolution.

2.4. *Results*

Figure 1 shows gray-scale maps of the number density, magnetic field lines, and β for model A at the times shown. A fast-mode shock is driven into the cloud, which reflects off the symmetry axis and returns to the edge of the cloud at the last time shown in Figure 1 (13.2×10^6 yr). At this point most of the cloud has $\beta \sim 0.03$ and is in the thermally unstable temperature range. Note that self-gravity can only have a minor effect on the dynamics up to this point since even at the latest time shown in the figure the free-fall time is $\simeq 3 \times 10^7$ yr, whereas the crossing time at the thermal sound speed is $\simeq 2 \times 10^7$ yr and that at the fast-mode speed is $\simeq 6 \times 10^6$ yr.

At this point the mean density of the cloud is $\simeq$30 cm^{-3}, which is typical of that in a GMC. Furthermore, the low value of β provides the ideal conditions for the generation of density inhomogeneities by MHD waves (Falle & Hartquist 2002), particularly since most of the gas is in the thermally unstable temperature range. The end result must be the formation of dense regions that are in the cold phase embedded in diffuse warm phase. Indeed, Figure 1 shows that such dense regions have already begun to form at the latest time shown. Unfortunately, we cannot follow the evolution of these dense regions much beyond this because not only does the numerical resolution become inadequate, but self-gravity begins to influence the large-scale dynamics of the cloud. However, it is clear that these regions will eventually come into approximate pressure

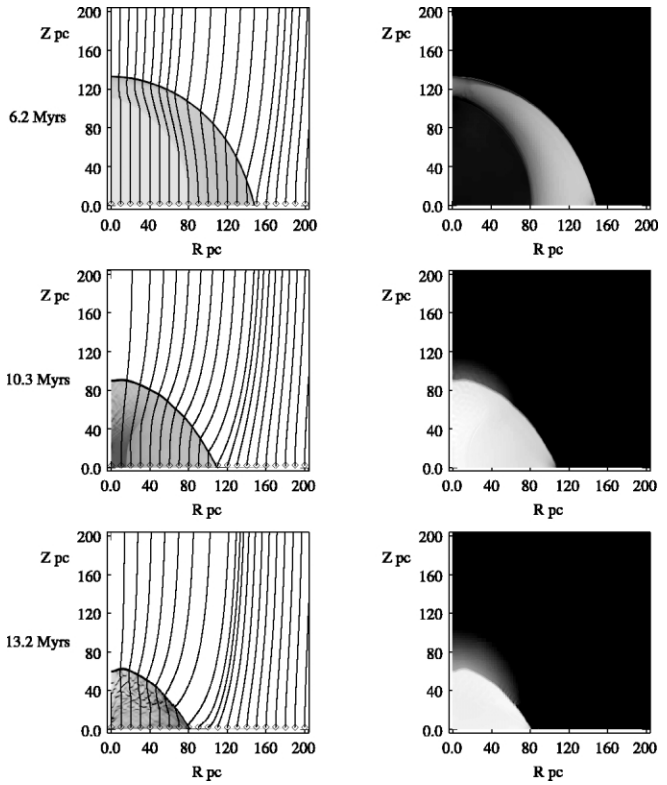

FIG. 1.—Linear gray-scale plots of the number density and magnetic field lines (*left*) and β (*right*) at the times shown. For the number density the range is 0–4, and for β it is 0–1.

equilibrium with the rest of the cloud, in which case their densities must be in the range 500–1000 cm^{-3}. This is typical of the densities in the translucent clumps in GMCs (e.g., Williams et al. 1995).

There is also a slow-mode shock that moves much more slowly than the fast-mode shock because the reduction in the magnetic pressure across it means that there is nothing to stop the gas being compressed as it cools, so that it comes into thermal equilibrium in the cold phase. This shock therefore produces a thin dense shell near the boundary of the cloud in which $\beta \simeq 1$. Since the postshock gas is in the thermally unstable regime, this process is unstable and we would expect the thin shell to fragment. Our calculations show that this does indeed occur at later times.

As one would expect, the increase in magnetic field inhibits collapse perpendicular to the field so that the cloud becomes flattened along the field lines. The slow shock must eventually eliminate the difference between the thermal pressures in the surroundings and the cloud so that it ends up as a thin disk in which β is of the same order as that in the surroundings. However, this process is not complete until $t \simeq 2.4 \times 10^7$ yr.

The behavior of the other simulations is similar, except that larger external pressures lead to faster evolution and smaller values of β. In order to quantify this, in Figure 2 we show the fraction of the volume of the cloud for which $\beta < 0.1$. It is clear that in all cases there is an extended period during which $\beta < 0.1$ in much of the volume of the cloud. Figure 3 shows that for models A and B, there is also a significant fraction of each cloud for which $\beta < 0.05$. The results for model E show that there is still a reasonable volume of low-β material even when the external thermal pressure decreases with time, although the timescale for this decrease must not be much smaller

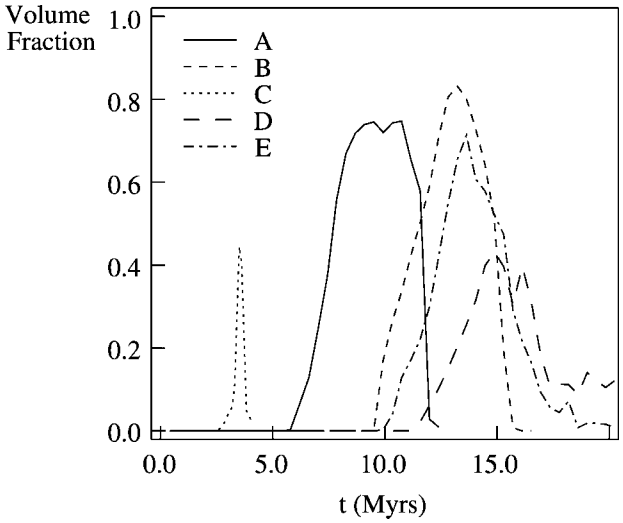

FIG. 2.—Fraction of the volume of the cloud for which $\beta < 0.1$.

than that in model E. For example, there is little low-β material when t_c is reduced to half this value.

Although a significant fraction of the volume of each cloud is occupied by material with low β, the corresponding mass fraction is somewhat lower. This is because, once the fast shock has returned to the cloud boundary, the cloud consists of three regions: the region interior to the slow shock, in which β is low and the gas is in the thermally unstable phase; the thin shell behind the slow shock, in which $\beta \simeq 1$ and the gas is in the cold phase; and a thin annulus on the symmetry plane, in which the conditions are similar to those in the thin shell. Although the thin shell and the annulus contain a significant fraction of the mass, they only occupy a small fraction of the volume.

The annulus is not very significant since it is an artifact of the symmetry of the calculation and would not be present in a more realistic calculation without this symmetry. On the other hand, a thin shell must appear in any such calculation. This is interesting since it is likely to break up into dense fragments (Koyama & Inutsuka 2000) and is therefore a possible site of star formation. In a more realistic simulation that is asymmetric due to an external flow, it would not be as regular as in our

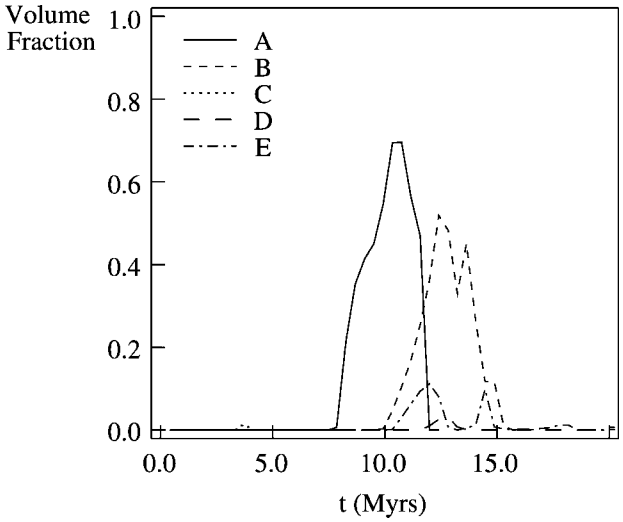

FIG. 3.—Fraction of the volume of the cloud for which $\beta < 0.05$.

simulation and so one might expect star formation to occur on one side of the cloud. There is a good deal of observational evidence that suggests that high-mass stars tend to form at the surfaces of GMCs (e.g., Israel 1978; Gatley et al. 1979: Fich et al. 1982). In the case of the Galaxy, this evidence is not conclusive, but observations of other galaxies may provide clearer results. For example, there is some tentative evidence from M33 that young high-mass stars are slightly offset from the molecular material (I. Pattison & M. G. Hoare 2005, in preparation).

3. CONCLUSIONS

The above simulations show the formation of highly magnetically dominated regions in thermally unstable material behind fast-mode shocks propagating through a cloud that is initially in a warm, thermally stable state. The external pressure variation required to generate such regions is well within the range expected in the midplane of the Galaxy. A slow-mode shock follows the fast-mode shock, leading to the production of dense regions in which the thermal and magnetic pressures are comparable. These dense regions may be the sites of high-mass star formation.

We thank L. Blitz and M. Hoare for input and the referee for helpful comments on the original version. A. J. L. acknowledges support from PPARC during the course of this work.

REFERENCES

Ballesteros-Paredes, J., Hartman, L., & Vasquez-Semadeni, E. 1999, ApJ, 527, 285
Ballesteros-Paredes, J., & Mac Low, M.-M. 2002, ApJ, 570, 734
Cox, D. P., & Smith, B. W. 1974, ApJ, 189, L105
Crutcher, R. M. 1999, ApJ, 520, 706
de Avillez, M. A., & Breitschwerdt, D. 2004, A&A, 425, 899
———. 2005, A&A, 436, 585
Dedner, A., Kemm, F., Kroner, D., Munz, C.-D., Schnitzer, T., & Wesenberg, M. 2002, J. Comput. Phys., 175, 645
Falle, S. A. E. G. 1991, MNRAS, 250, 581
Falle, S. A. E. G., & Giddings J. R. 1993, in Numerical Methods for Fluid Dynamics 4, ed. K. W. Morton & M. J. Baines (Oxford: Clarendon), 335
Falle, S. A. E. G., & Hartquist, T. W. 2002, MNRAS, 329, 195
Ferriere, K. 1998, ApJ, 497, 759
Fich, M., Treffers, R. R., & Blitz, L. 1982, in Regions of Recent Star Formation, ed. R. S. Roger & P. E. Dewdney (Dordrecht: Reidel), 201
Fiedler, R. A., & Mouschovias, T. Ch. 1993, ApJ, 415, 680
Gammie, C. F., Lin, Y.-T., Stone, J. M., & Ostriker, E. C. 2003, ApJ, 592, 203
Gatley, I., Becklin, E. E., Sellgren, K., & Werner, M. W. 1979, ApJ, 233, 575
Gazol-Patiño, A., & Passot, T. 1999, ApJ, 518, 748
Hartman, L. 2003, ApJ, 585, 398
Hennebelle, P., & Pérault, M. 1999, A&A, 351, 309
———. 2000, A&A, 359, 1124
Israel, F. P. 1978, A&A, 70, 769
Korpi, M. J., Brandenberg, A., Shukurov, A., Tuominen, I., & Nordlund, Å. 1999, ApJ, 514, L99
Koyama, H., & Inutsuka, S. 2000, ApJ, 532, 980
———. 2002, ApJ, 564, L97
———. 2004, ApJ, 602, L25
Mac Low, M.-M., Balsara, D. S., Kim J., & de Avillez, M. A. 2005, ApJ, 626, 864
McKee, C. F., & Ostriker, E. C. 1977, ApJ, 218, 148
Padoan, P., & Nordlund, A. 2002, ApJ, 576, 870
Sánchez-Salcedo, F. J., Vázquez-Semadeni, E., & Gazol, A. 2002, ApJ, 577, 768
Williams, J. P., Blitz, L., & Stark, A. A. 1995, ApJ, 451, 252
Wolfire, M. G., Hollenbach, D., McKee, C. F., Tielens, A. G. G. M., & Bakes, E. L. O. 1995, ApJ, 443, 152